Network 4 (1993) 285–294. Printed in the UK

Propagation of excitation in neural network models

M A P Idiart and L F Abbott

Department of Physics and Center for Complex Systems, Brandeis University, Waltham, MA 02254, USA

Received 26 April 1993

Abstract. We study the propagation of waves of excitation in neural network models. Through analytic calculation and computer simulation, we determine how the propagation velocity depends on the range and strength of synaptic interactions, the firing threshold and on transmission delays. For the models considered, the propagation velocity depends on either the first or the second moment of the distribution function characterizing the length of synaptic interactions.

1. Introduction

Under certain circumstances, stimulation of cortical or hippocampal tissue can produce a propagating wave of excitation [1]–[5]. Propagation velocities for such waves are of order 0.06 m s^{-1} in cortical slices [2] and 0.14 m s^{-1} in hippocampal slices [1]. This is much slower than the typical speed of action potential propagation along axons, which is more like 0.5 m s^{-1} [1]. The wave velocity is determined largely by population effects and it can be used to probe the nature of the connections between neurons [1]–[5]. However, to extract this information we must understand how the propagation velocity depends on the underlying synaptic connectivity. Propagation of waves of excitation was studied in [1] using a large network of conductance-based model neurons. Computer simulation of this network revealed that the propagation velocity was indeed sensitive to the spatial extent of network connections [1]. Here, we study the propagation of waves of excitation in much simpler neural network models. Although these models are not as realistic as that of [1], they have the advantage that we can derive analytic expressions for the wave velocity. This allows us to see what combination of parameters is actually being determined when the wave propagation velocity is measured. We calculate how the propagation velocity depends on the range of the synaptic connections, on threshold and maximal activities and on the axonal propagation velocity in these models and verify our results through computer simulation.

We consider neural network, or firing-rate, models of large neuronal populations [6]–[9]. In models of this sort, the activity at time t of neurons located at position x within the tissue is characterized by a variable $F(x, t)$. This function obeys a nonlinear differential equation relating the activity of neurons at point x to that of neurons located elsewhere, through synaptic interactions,

$$\tau \frac{dF(x,t)}{dt} = -F(x,t) + \int dy\, J(y) G[F(x+y,\ t-|y|/c)] \qquad (1.1)$$

where τ is a time constant. The function $J(y)$ characterizes the strength of the synaptic coupling between neurons located at the point x and those located at $x+y$. We have

0954-898X/93/030285+10$07.50

assumed translation invariance of the synaptic connections so that J does not depend on x. The function G is a nonlinear function of F that incorporates the dependence of synaptic transmission on the level of activity of the presynaptic neuron. In our preliminary analysis, we will keep the functions J and G fairly general. We normalize the synaptic weight function so that

$$\int dy\ J(y) = 1. \tag{1.2}$$

In (1.1) we have included a propagation delay. If the signal from neurons located at $x+y$ travels to the point x with velocity c, it will take a time $|y|/c$ to traverse this distance. This explains the factor $t-|y|/c$ in the function F in equation (1.1). The signal propagation speed c should not be confused with the speed of the waves of excitation we study, which we will denote by v. As mentioned above, v is normally considerably less than c.

In order to support a wave of excitation, equation (1.1) should have two spatially uniform, static solutions corresponding to a silent state, $F = 0$, and a firing or excited state, $F = F_e$. In order to support the $F = 0$ state, we must require that $G(0) = 0$. In fact, we will assume that G has a threshold so that $G(F) = 0$ for $F < \kappa$, where κ is the activity threshold for synaptic transmission. Likewise, we must have $G(F_e) = F_e$ to support the excited solution.

The waves we study involve transitions between these two states. Starting from the state $F = 0$, a region is stimulated raising F in that area to the excited, firing state. The excitation then spreads, increasing the size of the excited region. We are interested in determining how the velocity of this spreading wave of excitation depends on properties of the synaptic connection function $J(y)$ and the response function G.

2. General analysis

Our strategy for computing the propagation velocity v will be to impose a self-consistency condition on the activity function F. Suppose at some time t_0, and at some point x, there is no activity so that $F(x, t_0) = 0$. With this as an initial condition, we can integrate (1.1) over time to obtain

$$F(x,t) = \int_{t_0}^{t} \frac{ds}{\tau}\, e^{(s-t)/\tau} \int dy\ J(y) G[F(x+y,\ s-|y|/c)]. \tag{2.1}$$

We assume that $F(x, t)$ corresponds to a moving wave of activity. In equation (2.1), we will take t to be the time when the activity at point x first reaches the threshold value κ, so that $F(x, t) = \kappa$. Neurons at the point x were originally silent with $F(x, t_0) = 0$. The activity of other neurons already excited above the threshold increased F until it reached the threshold value κ at time t. This condition can be expressed in a form convenient for our calculations by substituting κ for the left side of equation (2.1) and integrating the right-hand side of the same equation by parts

$$\kappa = \int dy\ J(y) G[F(x+y, t-|y|/c)]$$

$$- \int dy\ J(y) \int_{t_0}^{t} ds\, e^{(s-t)/\tau} \frac{d}{ds} G[F(x+y, s-|y|/c)]. \tag{2.2}$$

Equation (2.2) is a self-consistency condition for the wave propagation velocity v. The wave must arrive at any given point just as that point rises above the threshold. This is

the basic equation we will use to compute the propagation velocity for waves of excitation. Note that in deriving equation (2.2) we only integrated the basic equation of the model (1.1) over the range $0 \leq F \leq \kappa$. This means that F only has to be described by equation (1.1) below the firing threshold. Once F crosses the threshold it could be described by a more complicated model and this would have no effect on our calculations. This is a very likely situation because many additional nonlinear processes become relevant once a neuron has crossed its firing threshold.

3. Analytical results for one dimension

The cortical and hippocampal slices used to measure propagation velocities [1]–[5] are very thin and are much smaller in the tranverse than in the longitudinal direction. For this geometry, the wave propagation is approximately one-dimensional. We look for solutions of equation (2.2) which are one-dimensional travelling waves moving in the positive x direction with velocity v

$$F(x,t) = f(t - x/v). \tag{3.1}$$

The function f has the general form shown in figure 1 with the asymptotic characteristics $f(-\infty) = 0$ and $f(\infty) = F_e$. By time-translation invariance we can specify f at any single time and position without loss of generality. We will make this choice so that at time $t = 0$, the point $x = 0$ is just reaching the threshold, that is $f(0) = \kappa$. We assume that f is monotonic so that $f(t) < \kappa$ for $t < 0$ and $f(t) > \kappa$ for $t > 0$.

To compute the propagation velocity, we substitute (3.1) into equation (2.2) and set $t_0 = -\infty$, $t = 0$ and $x = 0$. For $s < 0$, only negative y will contribute to the integral in equation (2.2), because for negative times the active part of the wave is in the negative spatial region. Thus, we can write

$$F(y, s - |y|/c) = f(s - \alpha y) \tag{3.2}$$

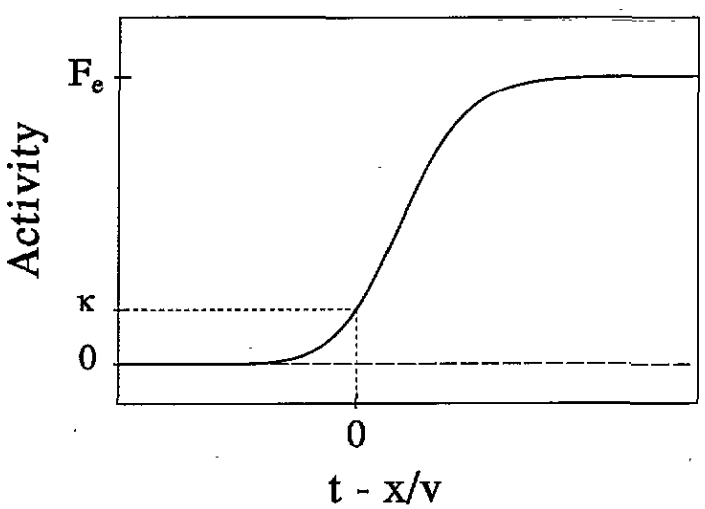

Figure 1. Typical shape of a one-dimensional travelling wave. The wave $f(t - x/v)$ crosses the threshold κ at $t - x/v = 0$ and satisfies $f(-\infty) = 0$ and $f(\infty) = F_e$.

where

$$\alpha = \frac{1}{v} - \frac{1}{c} \tag{3.3}$$

or equivalently

$$v = \frac{c}{1 + \alpha c}. \tag{3.4}$$

All of the effects of the finite signal velocity are contained in α. Note that since $v < c$, α is always bigger than zero. With these observations, equation (2.2) becomes

$$\kappa = \int_{-\infty}^{0} dy\ J(y)\left\{G[f(-\alpha y)] - \int_{-\infty}^{0} ds\ e^{s/\tau}\frac{d}{ds}G[f(s-\alpha y)]\right\}. \tag{3.5}$$

We will begin by calculating the propagation velocity when G is a simple step function, $G(F) = 0$ for $F < \kappa$ and $G(F) = F_e$ for $F > \kappa$. The wave arrives at the point $x = 0$ at $t = 0$, and at this time $F > \kappa$ with $G = F_e$ for $x < 0$ and $F < \kappa$ with $G = 0$ for $x > 0$. Since G jumps discontinuously at $F = \kappa$ and is otherwise constant, we have

$$\frac{d}{ds}G[f(s-\alpha y)] = F_e\delta(f(s-\alpha y) - \kappa)\frac{d}{ds}f(s-\alpha y) = F_e\delta(s-\alpha y) \tag{3.6}$$

where δ is the Dirac delta function. This makes the time integral in equation (3.5) trivial and we obtain

$$\kappa/F_e = \langle 1 - \exp(-\alpha|y|/\tau)\rangle \tag{3.7}$$

where we use the notation

$$\langle H(y)\rangle = \int_{-\infty}^{0} dy\ J(y)H(y) \tag{3.8}$$

for any function H.

The result (3.7) can be simplified if κ/F_e is small, that is, if the threshold level is much less than the maximum activity as it will be in our simulations. Then, we can expand the exponential in (3.7) to find

$$\alpha = \frac{\kappa\tau}{F_e\langle|y|\rangle} \tag{3.9}$$

or

$$v = \frac{cF_e\langle|y|\rangle}{F_e\langle|y|\rangle + c\kappa\tau}. \tag{3.10}$$

In the limit $c \to \infty$ this gives

$$v = \frac{F_e\langle|y|\rangle}{\kappa\tau}. \tag{3.11}$$

Thus, for a step function response with a big separation between the threshold and the maximal activity level, the propagation velocity depends on the first moment $\langle|y|\rangle$ of the synaptic distribution function J.

Now suppose that G is not a step function, but rises with some slope g at the threshold where

$$g = \left.\frac{dG(F)}{dF}\right|_{F=\kappa}. \tag{3.12}$$

Similarly, we define

$$h = \left.\frac{\mathrm{d}f}{\mathrm{d}t}\right|_{x=t=0}. \tag{3.13}$$

In some networks (see the simulations in the next section) neurons are excited to the threshold predominantly by other neurons that are near the threshold value. This occurs if the characteristic range of the synaptic interactions is much less than the distance that the wave moves while the activity rises from the threshold to its maximal value. In this case, f is near the threshold value over the range of y for which $J(y)$ is appreciably different from zero. For f near, but greater than the threshold, we can use the approximation (taking $y < 0$)

$$G[f(-\alpha y)] \approx gh\alpha|y| \tag{3.14}$$

and for $s - \alpha y > 0$

$$\frac{\mathrm{d}G[f(s-\alpha y)]}{\mathrm{d}s} \approx gh. \tag{3.15}$$

Substituting these results into equation (3.5) gives

$$\frac{\kappa}{gh\tau} = \frac{\alpha\langle|y|\rangle}{\tau} + (\exp(-\alpha|y|/\tau) - 1). \tag{3.16}$$

To simplify this expression, we can assume once again that the threshold κ is small, in this case compared to $gh\tau$. Then, the exponential can be expanded to give the approximate equation for α,

$$\frac{\kappa}{gh\tau} = \frac{\alpha^2\langle y^2\rangle}{2\tau^2} \tag{3.17}$$

so that

$$v = \frac{c(gh\langle y^2\rangle)^{1/2}}{(gh\langle y^2\rangle)^{1/2} + (2\kappa\tau)^{1/2}c}. \tag{3.18}$$

In the limit $c \to \infty$ this gives

$$v = \left(\frac{gh\langle y^2\rangle}{2\kappa\tau}\right)^{1/2}. \tag{3.19}$$

Note that the velocity now depends on the second moment of J, $\langle y^2\rangle$.

4. Numerical simulations

To perform computer simulations of the waves we are studying, we use a model with discrete spatial elements and write (1.1) as

$$\tau\frac{\mathrm{d}F_i(t)}{\mathrm{d}t} = -F_i(t) + \sum_j J_{ij}G[F_j(t)]. \tag{4.1}$$

We do not include any transmission delay in our simulations so $c \to \infty$. We consider a one-dimensional open chain of N neurons. The first model we investigate uses a synaptic response function given by [9]

$$G[F_j(t)] = \tanh[g(F_j(t) - \kappa)]\Theta(F_j(t) - \kappa) \tag{4.2}$$

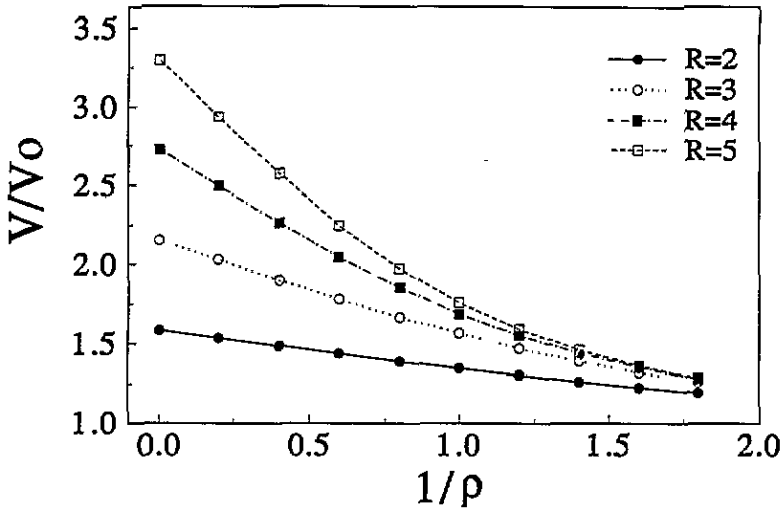

Figure 2. The ratio of the wave velocity to the velocity with nearest neighbour coupling for the model of [9] plotted as a function of the inverse of the synaptic range ρ for different values of the synaptic cutoff length R. The threshold was $\kappa = 0.001$ and $g = 1.3$. Distances are measured in units of the interneuron spacing.

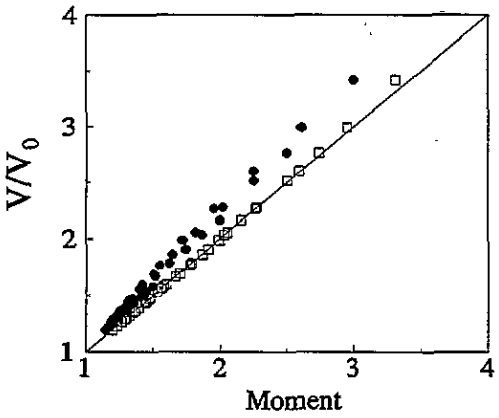

Figure 3. The same data as in figure 2 plotted as functions of either the first moment $\langle|y|\rangle$ (solid dots) or the square root of the second moment $(\langle y^2\rangle)^{1/2}$ (open squares) of the synaptic distribution function J. Distances are in units of the interneuron spacing.

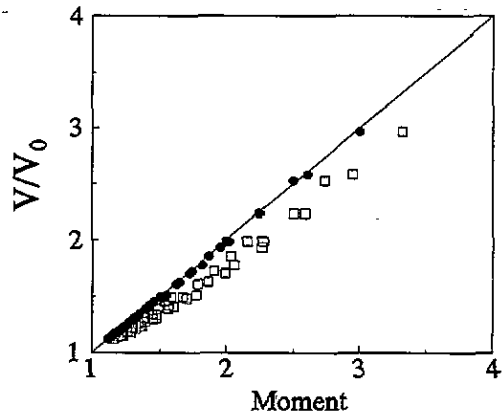

Figure 4. The same plot as in figure 3, but with $g = 100$ and $\kappa = 0.05$. The velocity ratio is plotted as functions of the first moment $\langle|y|\rangle$ (solid dots) and the square root of the second moment $(\langle y^2\rangle)^{1/2}$ (open squares) of J and distances are in units of the interneuron spacing.

where Θ is the unit step function. The synaptic connections we consider have a maximum range R and an exponential fall-off with a length constant ρ so that

$$J_{ij} = J_0 e^{-|i-j|/\rho}\Theta(R - |i-j|)\,. \tag{4.3}$$

J_0 is determined by the condition $\sum_j J_{ij} = 1$.

Our simulation procedure consists of injecting a constant current (added to the right-hand side of equation (4.1)) for a certain time interval into the first neuron of the chain.

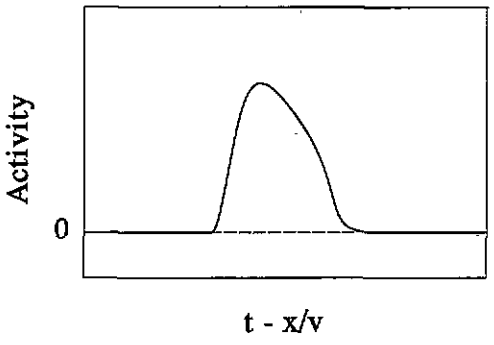

Figure 5. Shape of the travelling wave for the more complex model simulated [8]. Inhibition causes the pulse of excitation to terminate in a finite time.

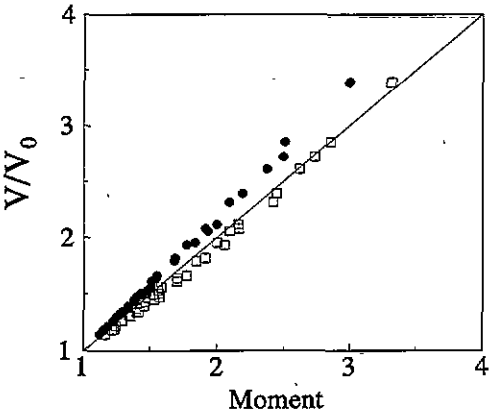

Figure 6. Similar to figures 3 and 4 but data are from the model with inhibition [8]. The velocity ratio is plotted as a function of the first moment $\langle|y|\rangle$ (solid dots) or the square root of the second moment $(\langle y^2\rangle)^{1/2}$ (open squares) of J and distances are in units of the interneuron spacing.

If the intensity and the duration of this pulse are sufficient, the next neuron starts to fire and a wave of activity travels along the chain until all the neurons are active. We determine the velocity of this wave by measuring the difference in time between the arrival of the activity at two distant neurons. We hold $N = 100$ and $\tau = 1$ fixed and investigate the behaviour of v by modifying the length constant ρ and the cut off R for several choices of the gain g and threshold κ.

Figure 2 shows a typical example, a plot of the propagation velocity against the inverse of the synaptic length constant ρ for different length cutoffs R. For convenience, we have divided the velocity v in the figures by v_0, the velocity for nearest neighbour coupling, that is, the monosynaptic velocity [1]. This is convenient because, in the limit we consider, this ratio primarily depends on properties of the synaptic coupling function J. Figure 2 shows that a more distributed J_{ij} gives a higher velocity.

Using what we learned from the previous section, we can display this data in a clearer way. For the parameters we have chosen (the same as those used in [9]), the conditions of the second computation of the previous section are satisfied and we expect the wave velocity to be proportional to the square root of the second moment of J, $(\langle y^2\rangle)^{1/2}$. The ratio v/v_0 should, in fact, be equal to $(\langle y^2\rangle)^{1/2}$ because the constant of proportionality cancels out. Figure 3 shows the results for $g = 1.3$ and for $R = 2$, 3, 4 and 5 plotted against both $(\langle y^2\rangle)^{1/2}$ and $\langle|y|\rangle$. We observe that, to a very high degree of accuracy, v/v_0 is indeed equal to $(\langle y^2\rangle)^{1/2}$ in accordance with equation (3.19). In particular, v/v_0 does not depend on ρ and R separately but only through their combined effect on the second moment of J. When these data are plotted against the first moment of J, $\langle|y|\rangle$, the data do not fall along the diagonal and we get more scatter on the plot (figure 3). The scatter indicates that the velocity ratio cannot be expressed as a function solely of $\langle|y|\rangle$. We get similar results for a variety of parameters as long as g is not too large.

For large values of g, the hyperbolic tangent approaches a step function and we expect to find the first moment dependence discussed in the last section. This is seen in figure 4, where, with $g = 100$, the fit of the velocity to $\langle|y|\rangle$ is excellent while the plot of v/v_0

against $(\langle y^2 \rangle)^{1/2}$ is scattered and off the diagonal.

We also simulated a more complex model with explicit inhibition [8]. This model includes the effects of both fast (GABA-A) and slow (GABA-B) inhibition. The fast inhibition regulates the firing rate during excitation while the slow inhibition brings the system back to the silent state after a period of excitation [8]. As a result, the wave now has the profile shown in figure 5. In figure 6 we present the results of a series of simulations similar to what we described for the previous model. The fit to the square root of the second moment of the synaptic distribution is not as good as it was in figure 3, but it still provides an adequate description of the data. The fit to the first moment dependence is not as good.

5. Two-dimensional propagation

For wave propagation in a portion of intact cortex, a two-dimensional model is more appropriate than the one-dimensional analysis we used for slices. (We assume we can still ignore variations across the thickness of the cortex. Otherwise, of course, a full three-dimensional model must be used.) If the stimulus is independent of one of the two dimensions, the previous results can be taken over with J replaced by its one-dimensional analogue

$$J^{\text{eff}}(y_1) = \int \mathrm{d}y_2 \, J(\boldsymbol{y}). \tag{5.1}$$

However, this is an unlikely situation since the diameter of the electrode that injects current into the tissue is typically quite small. Instead of seeing a plane wave, we would expect a circular wave to originate at the site of the electrode and to spread outward.

For simplicity, we consider only circular waves and assume that the synaptic interaction function J is isotropic, $J = J(|\boldsymbol{y}|)$. The circular wave, once initiated, expands with an ever increasing velocity that ultimately approaches the velocity of a plane wave. We choose coordinates with the origin at the centre of the circular wave and define the wave radius r to be the radius where the activity is equal to the threshold, $F = \kappa$. The propagation velocity $v(r)$ is the velocity of this wave front when it has radius r. As we saw in the one-dimensional model, the velocity of a wave of excitation is governed by the time it takes the advancing wave to raise neurons in its path to the firing threshold. Let R be the maximum radius of synaptic interactions as in the previous section. The region of the two-dimensional space that contributes to raising neurons at the point $\boldsymbol{x}$ above the threshold is the intersection of the circular region of radius $r = |\boldsymbol{x}|$ where $F > \kappa$ and another circle of radius R around the point $\boldsymbol{x}$ (see figure 7). It is clear that as the circular wave grows this overlap region will grow, increasing the velocity of the wave.

Our next step is to extract analytical results for the velocity of a circular wave in two-dimensions. We have not solved this problem exactly, but we can derive some interesting bounds on this velocity. The first bound has already been discussed. If we define $v(\infty)$ as the velocity of a plane wave or, equivalently, of a circular wave with infinite radius, then for a circular wave of finite radius we have $v(r) < v(\infty)$. To derive a lower bound, we begin by considering a step function response, $G = 0$ for $F < \kappa$ and $G = F_e$ for $F > \kappa$. In this case, we can derive a result similar to (3.6)

$$\frac{\mathrm{d}}{\mathrm{d}s} G[F(\boldsymbol{x}+\boldsymbol{y}, s)] = F_e \delta(F(\boldsymbol{x}+\boldsymbol{y}, s) - \kappa) \frac{\mathrm{d}}{\mathrm{d}s} F(\boldsymbol{x}+\boldsymbol{y}, s) = F_e \delta(s - T(\boldsymbol{x}+\boldsymbol{y})) \tag{5.2}$$

where $T(x+y)$ is defined as the time when the region at point $x+y$ reaches the threshold, that is, $F(x+y, T(x+y)) = \kappa$. Putting this into equation (2.2) we find

$$\frac{\kappa}{F_e} = \int_{A(r)} dy\ J(|y|)\left(1 - e^{(T(x+y)-t)/\tau}\right). \tag{5.3}$$

Here $A(r)$ is the area shown in figure 7, where the range of synaptic interactions from the point x overlaps with the region of firing ($F > \kappa$) at time t when the wave has radius r.

Unfortunately, to evaluate the integral in (5.3) we need to know the function T which is, of course, the answer we seek. However, note that $t - T(x+y)$ is the time it takes for the wave to expand from a radius $|x+y|$ to the radius $r = |x|$. This time is always greater than the time it would take the wave to expand this much if it had a constant velocity $v(r)$, $(r - |x+y|)/v(r)$, because the velocity of the circular wave for times less than t is always less than $v(r)$. Since the integrand in (5.3) is an increasing function of $t - T(x+y)$, we can write

$$\frac{\kappa}{F_e} > \int_{A(r)} dy\ J(|y|)\left(1 - e^{(|x+y|-r)/v(r)\tau}\right). \tag{5.4}$$

In evaluating the right-hand side of equation (5.4), we find it best to express the answer in terms of the asymptotic velocity $v(\infty)$. If we take the limit $r \gg R$ we find that

$$v(\infty) > v(r) > v(\infty) - \frac{F_e}{4\kappa\tau r^2}\int_0^R dy\ y^4 J(y). \tag{5.5}$$

The same arguments can be applied when G is not a step function if we take advantage of the approximations we used in the one-dimensional analysis. If F stays near the threshold in the region of interest, we can write (for $|x+y| < r$)

$$G[F(|x+y|, t)] = gh(t - T(x+y)) > gh(r - |x+y|)/v(r) \tag{5.6}$$

and use equation (3.15). Making the same approximations as before we find

$$\frac{\kappa}{gh\tau} > \int_{A(r)} dy\ J(|y|)\left(\frac{r - |x+y|}{v(r)\tau} + e^{(|x+y|-r)/v(r)\tau} - 1\right). \tag{5.7}$$

Again taking $r \gg R$ we obtain the bounds

$$v^2(\infty) > v^2(r) > v^2(\infty) - \frac{gh}{24\kappa\tau r^3}\int_0^R dy\ y^6 J(y). \tag{5.8}$$

Note that, in this case, the correction for finite radius falls off more rapidly than for a step-function response.

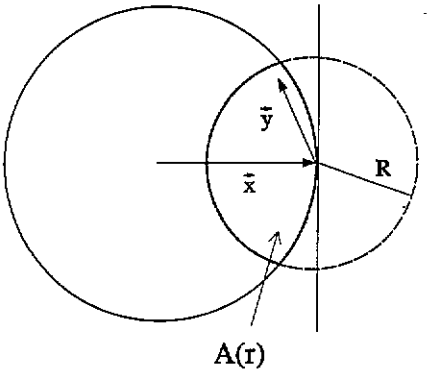

Figure 7. Area of overlap for the two-dimensional calculation. The vector x marks the point in question and also the radius of the circular wave at time t. The circle of radius R is the range of synaptic interactions. The overlap of the two circles with area $A(r)$ is the region used in the computation of the wave velocity.

6. Conclusions

We have shown that, with a few general assumptions about the differential equations that determine the neuronal dynamics in a network, it is possible to derive relatively simple relations between the propagation velocity of a excitatory wave and the spatial distribution of synaptic connections. Two limiting cases give quite different behaviour. If the range of synaptic interactions is much greater than the distance that the wave travels in the time it takes to rise to its maximal activity, the synaptic response acts effectively like a step function and the wave velocity is given by equation (3.7). When the ratio of the threshold activity to the maximal activity is small, this gives a velocity that depends on the first moment of the synaptic distribution function, $v \propto \langle |y| \rangle$. If instead, neurons are excited primarily by other neurons that are still near the threshold value during the rising phase of their activity, the velocity is given by equation (3.16) and, in the limit of small threshold, $v \propto (\langle y^2 \rangle)^{1/2}$. The two different dependences were clearly revealed in the computer simulations. Our bounds for the velocity of two-dimensional propagation provide a first step toward a solution of this more difficult problem.

Acknowledgments

This research was supported by CNPq (Brazilian Agency) and National Science Foundation grant DMS-9208206.

References

[1] Miles R, Traub R D and Wong R K S 1988 Spread of synchronous firing in longitudinal slices from the CA3 region of the hippocampus *J. Neurophysiol.* **60** 1481–96

[2] Chervin R D, Pierce P A and Connors 1988 B W Periodicity and directionality in the propagation of epileptiform discharges across neocortex *J. Neurophysiol.* **60** 1695–713

[3] Goldensohn E S and Salazar A M 1986 Temporal and spatial distribution of intracellular potentials during generation and spread of epileptogenic discharges *Basic Mechanisms of the Epilepsies, Advances in Neurology* ed A V Delgado-Escueta, A A Ward, D M Woodbury and R J Porter (New York: Raven)

[4] Gutnick M J and Wadman W J 1986 Intrinsic neuronal connectivity in neocortical brain slices as revealed by non-uniform propagation of paroxysmal discharges *Soc. Neurosci. Abstracts* **12** 349

[5] Knowles W D, Traub R D and Strowbridge B W 1987 The initiation and spread of epileptiform bursts in the in vitro hippocampal slice *Neuroscience* **21** 441–55

[6] Wilson H R and Cowan J D 1972 Excitatory and inhibitory interactions in localized populations of model neurons *Biophys. J.* **12** 1–24

[7] Hopfield J J 1984 Neurons with graded response have computational properties like those of two-state neurons *Proc. Natl Acad. Sci.* **81** 3088–92

[8] Abbott L F 1991 Firing-rate models for neural populations *Neural Networks: From Biology to High-Energy Physics* ed O Benhar, C Bosio, P Del Guidice and E Tabet (Pisa: ETS Editrice) pp 179–96

[9] Amit D J and Tsodyks M V 1990 Quantitative study of attractor neural network retrieving at low spike rates I and II *Network* **2** 259–94; 1991 Effective neurons and attractor neural networks in cortical environment *Network* **3** 121–38